Multiscale assessment of structured coated abrasive grits in belt finishing process

Kévin Serpin [a,b,*], Sabeur Mezghani [a], Mohamed El Mansori [a]

[a] Arts et Métiers Paris Tech, MSMP – EA 4106, Rue Saint Dominique, BP 508, 51006 Châlons-en-Champagne, Cedex, France
[b] RENAULT S.A.S., Direction de l'Ingénierie de la Production Mécanique, Avenue du Golf, 78280 Guyancourt, France

A B S T R A C T

This paper outlines the link between grit morphology and surface roughness of belt-finished workpieces. It features a comparative analysis of a new generation of abrasive belts with diverse abrasive structures, and a multi-scale roughness characterization of abrasive belt wear on a variety of finished surfaces. The ultimate thickness of the mechanically deformed layer and surface profile projections depends, to a great extent, on the abrasive mechanisms of friction and wear employed in the finishing process. By modifying the physical mechanisms (cutting, plowing or sliding), it is possible to achieve a concomitant change in the rate of material removal and, consequently, to the specific surface roughness of the finished parts.

Our research shows that the active roughness scale resulting from belt finishing is strongly dependent on the grit orientation and the binder distribution. The results are promising for increasing the efficiency of the abrasion processes and for improving the surface texturing of finished parts.

Keywords:
Belt finishing
Wear
Abrasion
Multiscale analysis

1. Introduction

The main objectives in the automotive industry for the improvement of environmental efficiency in vehicle engines are to reduce oil consumption and to limit noxious emissions. Various manufacturing processes are used to achieve this goal, which are generally based either on using lightweight material to reduce load, reducing heat losses due to exhaust and conduction through engine body, or by improving the frictional loss in the mechanical contact, particularly inside the engine [1].

In a passenger car engine, about 30% of the total frictional loss is accounted for by the bearings alone [2]. One of the ways to reduce friction is to act on surface morphology. In practice, this is achieved by using anti-friction coating technologies, texturation technology like in the honing process, or more traditionally, by reducing surfaces roughness. Nowadays, on passenger car crankshafts, the latter option is the most commonly employed. The process engineering departments have to maintain specific geometrical specifications and a very strict surface finish. Moreover, high volume production and cost reduction requires the utmost efficiency in the manufacturing process, especially for finishing and superfinishing operations.

In this regard, the advanced belt finishing process is remarkably simple and inexpensive [3]. Its principles of operation are well known: pressure-locked shoe-platens circumferentially press an abrasive coated belt on a rotated workpiece. This abrasive machining process is used extensively in the automotive industry to superfinish crankshaft journals and pins, which allows for the reduction of surface irregularities, improves the geometrical quality, and increases wear resistance and fatigue life. However, one of the major industrial issues with this manufacturing process is its efficiency and robustness. The superfinishing of crankshaft journals and pins is generally achieved by processing three steps of belt-finishing while successively decreasing the grits' size, which involves substantial manufacturing costs.

One of the most promising ways to reduce this cost is by controlling the distribution and morphology of the abrasive grits. Recently, a new generation of abrasive belts coated with structured and shaped agglomerated grits has become commercially available. These belts promise to be more efficient and would have a better wear resistance compared to the traditional coated abrasive belts. The present study aims to analyze these new belts and to investigate the link between their morphologies, the surface finish of belt-finished workpieces, and the physical mechanisms which govern their wear performance.

2. Experimental procedure

In this work, the belt structure is qualitatively characterized by SEM observations before and after belt finishing operations. Then,

* Corresponding author. Tel.: +33 326 69 91 66; fax: +33 326 96 91 97.
E-mail address: kevin.serpin@renault.com (K. Serpin).

http://dx.doi.org/10.1016/j.wear.2015.01.054

Nomenclature

t_c	cycle time (s)
D	initial workpiece diameter (mm)
R	initial workpiece radius (mm)
L	belt finished width (mm)
E_s	total specific energy (J mm^{-3})
ΔP	power of the belt finishing machine (W)
ΔV	removal volume (mm^3)
Δh	removal thickness (μm)
R_{pk}	reduced peak height (ISO 13565) (μm)
R_k	core roughness depth (ISO 13565) (μm)
R_{vk}	reduced valley depths (ISO 13565) (μm)
R_z	maximum height of roughness profile (ISO 4287) (μm)
$Mr1$	material portion corresponding to the upper limit position of the roughness core profile (ISO 13565) (%)
$Mr2$	material portion corresponding to the lower limit position of the roughness core profile (ISO 13565) (%)
M_a	multiscale arithmetic roughness average (μm)
MPS	Multiscale Process Signature

the effect of the abrasive belt structure on roughness is identified using standard functional parameters and a multi-scale analysis in a wide-scale range. An energy analysis is applied to identify the cutting ability related to the abrasive structure of the coated belts. Finally, a global belt finishing process efficiency analysis is conducted to discuss the functional relevance of each belt structure.

The test rig consists of a conventional lathe, a belt finishing apparatus, and a power transducer allowing the measure in-situ of the power dissipated during the superfinishing process. The belt finishing apparatus is composed of two horizontal arms equipped with special pressure assisted shoe-platen (see Fig. 1).

With this type of shoe-platen, each insert can be moved in a radial direction by hydraulic cylinders pressing the abrasive belt against the periphery of the workpiece with a locally known value of the contact pressure. One of the benefits of this technology is its flexibility since belts with different thicknesses can be fit on the shoe-platens without significantly changing the contact surface between inserts and workpiece, which is not the case when traditional shoe-platens with motionless inserts are used. Since the feed pressure of the hydraulic cylinders is the same, a constant pressure distribution is obtained along the abrasive belt/workpiece contact angle (approximately 320°). This pressure value does not change during the process and it can be easily controlled using the feed pressure of cylinders in the shoes. The tests are performed on wet conditions varying the abrasive belt structure while other working parameters are kept constant (see Table 1).

Four types of structured abrasive belts with the same grits size range (about 30 μm) are considered in this study. The different belt structures studied are as follows:

- *Type I:* A common structure often used to superfinish crankshaft journals and pins (see Fig. 2(a)). The abrasive belt is constituted of a large amount of calibrated grits electrostatically deposited on a polyester backing coated by a layer of synthetic or water based resin. With this deposition process, the grits are oriented perpendicularly to the backing and their cutting edge offers an important material removal capacity. Moreover, this kind of belt can have an anti-slip layer on the backside, which allows for a better hold of the belt during the belt finishing operations. Three belt models with this structure (5902, 372 L and 272 L) are considered.
- *Type II:* A structure composed of lapped grits (see Fig. 2(b)). The abrasive belt is constituted of grits partially or completely covered by resin. The cutting edges are flattened, well oriented, and less aggressive.
- *Type III:* A shaped structure constituted by a thick web backing on which is deposited half-spherical agglomerates (see Fig. 2 (c)). Each half-spherical structural element is composed of 30 μm grits bounded together by a resin. The grit density is very high as compared to the other structures considered. In addition, this belt type has a small contact area between the abrasive structure and the surface of the workpiece.
- *Type IV:* A shaped structure constituted by a plasticised web backing on which pyramidal agglomerates are deposited (see Fig. 2(d)). Each pyramid has a square base and is constituted of 30 μm grits bound together by a resin. As with the Type III belts, only the summits are in contact with the workpiece.

Table 1
Belt finishing working conditions.

Workpiece rotation speed	100 rpm
Normal force of the shoe-platens	600 N
Oscillation frequency of shoes	265 cycles per min
Oscillation amplitude of shoes	1 mm
Cycle time	12 s
Lubrication fluid	Neat oil
Feedrate of the abrasive belt	None

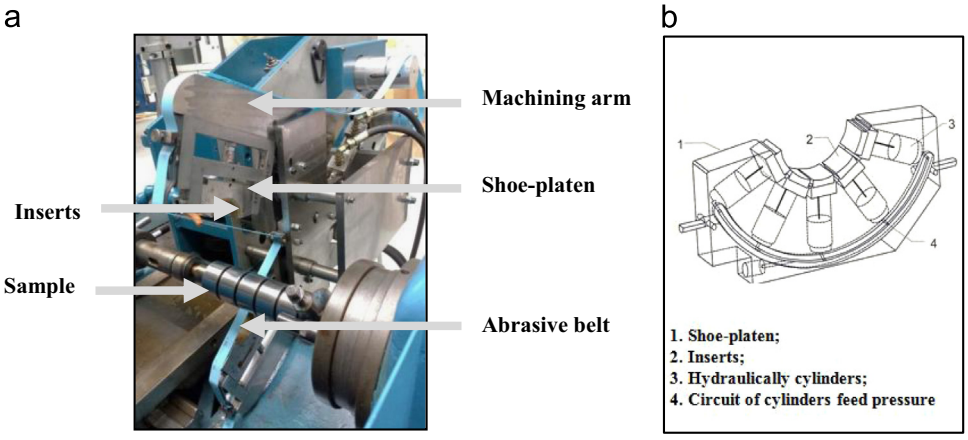

Fig. 1. Belt finishing apparatus (a) and pressure assisted shoe-platen (b).

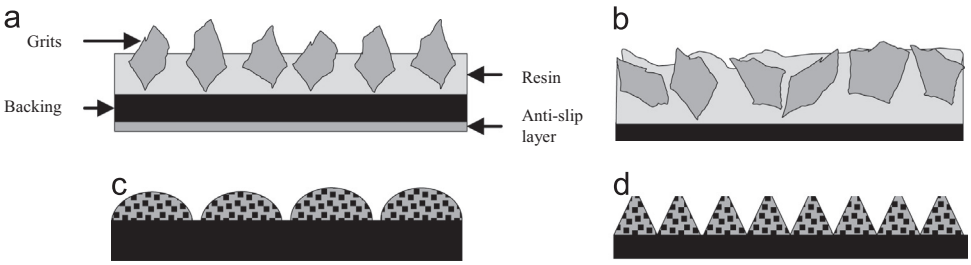

Fig. 2. Four structures of abrasive belts; 5902, 372L and 272L (a), 261X (b), 2970 (c), and 253FA (d).

Table 2
Characteristics of the abrasive belts considered in this study.

Type	Grits size	Model	Supplier	Grits	Deposition	Backing
I	≈ 30 μm	5902	SIA	Al_2O_3	Electrostatic	Polyester
I	≈ 30 μm	372L	3M	Al_2O_3	Electrostatic	Polyester
I	≈ 30 μm	272L	3M	Al_2O_3	Electrostatic	Polyester
II	≈ 30 μm	261X	3M	Al_2O_3	Lapping	Polyester
III	≈ 30 μm	2970	SIA	Al_2O_3	Flattening	Web
IV	≈ 30 μm	253FA	3M	Al_2O_3	Micro-replication	Web

The characteristics of the coated abrasive belts used in this study are shown in Table 2.

The tests were repeated three times for each belt model. The effects on the belt finishing performances were studied on steel samples whose characteristics are given in Table 3.

The average power absorbed during the belt finishing process is calculated as the average difference between on-load powers recorded during the finishing and off-load power recorded before and after the tests. Geometrical and superficial variations of the workpiece samples were measured using a 2D Surfascan apparatus. The tip radius of the diamond stylus is 2 μm. The surface micro-profile on each specimen was taken along the axial direction over a sampling length of 16, and 8 mm and at three equally spaced circumferential locations. Measurements were carried out before and after the belt finishing tests. Furthermore, SEM observations of abrasive belts morphologies were performed, also before and after the belt finishing tests. The worn abrasive belts were then cleaned by an ultrasonic bath before SEM analysis.

3. Results and discussions

3.1. Abrasive belt wear characterization

The assessment of coated abrasive properties for the use in belt finishing is a complex problem due to the variation of grit morphology from particle to particle [4]. In order to analyze the grits' characteristics and to better understand the activated physical phenomena, we performed SEM micrographs of the belt surface morphology (see Fig. 3). Notice that the 2970 belt micrographs have been taken at the summit of the half-spherical structural elements.

Overall, the total grit size is different from the visible grit size. This is mainly due to the depositing process by which the grits are more or less inserted into the resin. Even on the same belt, the exposed part of the grits can greatly vary. For example, we observe differences in the grits' appearance between the initial Type I belts (5902, 372L and 272L). The 5902 model has voluminous grits and their cutting edges appear less sharp than in the 372L and 272L models. Moreover, we note that the 5902s density is the highest of the Type I models. The grits' orientation is also different. The 272 L's grits seem to be more evenly spread over the resin while 372L's grits have the sharpest cutting edges.

The Type II (261X) belt's initial micrograph shows a structure with grits partially or completely covered by the resin. The waviness distinguished here corresponds to the underlying grits' distribution. Globally, the 261X's grits offer slanting cutting edges.

This orientation is also observed on the Type III belt (2970). Concerning the latter, the resin is not visible and the grit meshing appears highly compact.

Finally, the pyramidal shapes of the Type IV (253FA) belt can be observed on the last micrograph. The square base of each pyramid is about 500 μm^2. In addition, we remark that the visible size of grits constituting the pyramidal structures is very variable and ranges from several μm to about 30 μm.

By analyzing the state of belts after belt finishing, we observe that the wear of Type I belts leads to a partial or total loosening of the most prominent grits. This phenomenon depends on the grits' characteristics (indentation depth, orientation, angle of the cutting edges, volume, etc.) and on the applied forces. An attentive eye will note the presence of small cracks starting from the grits/resin interface. This undoubtedly represents the first step of the grits loosening. Qualitatively, after analyzing a large area of the belt, the loosening mechanism is more pronounced for 5902 and 372L belts than for the 272L. This can be linked to the high grit density with less active cutting edges.

Abrasion causes an important resin removal on the Type II belt. We notice the flattening of the resin and the emergence of new cutting edges which initially were totally covered. Furthermore, no grit extrusion is observed.

On the Type III belt, the chip generation has completely obstructed the interstice between the grits, despite the preliminary cleaning operation. The grits' cutting edges seem to be entirely covered by metallic chips. This would indicate that the grits' density has prevented the chips from becoming dislodged. The cutting ability of the belt has undoubtedly been deteriorated. Once again, there is no grit extrusion.

Finally, the Type IV belt's post process micrograph shows that only the summits have been worn. Thanks to its structure, the abrasion renews the belt's grits by creating new cutting edges and preserves the cutting ability. This belt type thus offers better durability than the classic belts (Type I) whose grits are loosened quickly and where the sharp cutting edges rapidly become rounded.

3.2. Workpiece surface finish

To give an estimate of the surface finish improvements, the gain ratio of the functional roughness parameters R_{pk}, R_k and R_{vk} (ISO 13565 standard) have been assessed. They are based on the analysis of a bearing curve (the Abbott–Firestone curve), which is simply a plot of the cumulative probability distribution of surface

Table 3
Workpiece characteristics before belt finishing test.

Workpiece material	D38MSV5S Steel (%C 0.35/0.40)
Diameter D	54.8 ± 0.005 mm
Belt finished width L	20 mm (belt width) +2 mm (oscillations' amplitudes)
Fabrication steps	Turning, induction hardening, grinding, 80 μm belt finishing
Superficial hardness	≈ 55 HRC
Initial roughness	Average R_a: 0,437 μm (± 0.048 μm)

roughness height [5]. These parameters are particularly relevant when characterizing textured surfaces. R_{pk} is the average height of protruding peaks above the roughness core profile. R_{vk} is the average depth of valleys projected through roughness core profile. R_k is the average height of the protruding peaks above the roughness core profile.

The following equation describes the expression of gain ratios for each parameter:

$$\Delta X(\%) = 100 \times \frac{X^{initial} - X^{final}}{X^{initial}} \quad (1)$$

X can represent R_{pk}, R_k or R_{vk}. The average gain ratios have been calculated for the considered parameters for each belt model. The results are given in Fig. 4.

The Type I, Type II and Type IV belts enable a good peak clipping (the final R_{pk} is about 80% lower than the initial R_{pk}). The belt with the pyramidal structure (Type IV) shows low process variability and high surface finish repeatability. In fact, the R_{pk} parameter presents the lowest variability. The belt with lapped grits (Type II) has the particularity of preserving valley depth while reducing roughness peaks and core. This ability can be interesting in an antifriction strategy where bearing surfaces must have the least asperities but an important retention capacity in order to well irrigate the contact in lubricant (particularly in a boundary and mixed lubrication regime). Finally, the functional roughness gain ratios with the Type III belt follows the same trend as the Type II belt, in which valley depths are less reduced. However, the Type III belt has the poorest repeatability. This behavior can be explained by the high chip accommodation of this structure during belt finishing.

3.3. Multiscale surface finish analysis

In order to quantify the impact of each structure of coated abrasive belts at all surface finish scales, we investigated the signature of the belt finishing process in a wide range of topographical scales before and after finishing with the 1D discrete wavelet transform on eight decomposition scale levels. The surface profiles pass through a filter bank which is a set of contracting wavelets obtained from a unique wavelet function by translation and dilatation.

The methodology consists of the extraction of each scale by inverse wavelet transform, and hence, on the quantification of their arithmetic mean values. In fact, the idea is to determine the spectrum of arithmetic mean value from the scales of waviness to roughness M_a [6–8]. This approach allows us to determine the multiscale transfer function of the morphological modification in surface topography after the belt finishing process. This transfer function is denoted as the Multiscale Process Signature (*MPSi* (%)) and is obtained by calculating the M_a gain ratio according to the following equation:

$$\mathrm{MPS}_i(\%) = 100 \times \frac{{M_a}^{initial}(i) - {M_a}^{final}(i)}{{M_a}^{initial}(i)} \quad (2)$$

The first step of this analysis is to choose a relevant wavelet filtering function necessary to decompose the initial profile signal. In order to identify this criterion we have decomposed the profile signals, before and after belt finishing with six different wavelets. The average MPS is then calculated on each scale. Fig. 5(a, and b) shows an example of the effect of wavelet function relative to the surface belt-finished with the 5902 belt.

We note a very low dispersion of the MPS, particularly in roughness scales lower than 512 μm. Moreover, the relevance to characterize the appropriate scales of surface finish by abrasion does not depend on the shape of the wavelet, as demonstrated in [9]. Subsequently, the decomposition using the "db2" wavelet is considered. Fig. 6(a, and b) represents the results obtained by the multiscale analysis of the roughness profiles of each abrasive belt model.

It appears on Fig. 6(a) that the surface roughness level depends on the contact scale. The Type I (5902, 272L and 372L) and Type IV (253FA) belts offer the best improvement in MPS irrespective of the scales. We can distinguish two behaviors in accordance with the characteristic scale. The first behavior is a increase in the MPS gain ratio up to the scale of about 512 μm. Below this scales (micro-roughness), the roughness reduction is very high up to 80%. For higher scales (macro-roughness and waviness), a rapid decrease of the gain ratio is observed. This means that these belts perform best on fine roughness scales and much less on the large ones.

Concerning the Type II belt (261X), the roughness reduction is not uniform in scale range. In fact, the MPS decreases from small scales to large scales. Furthermore, the MPS amplitude is significantly lower than the Type I and Type IV belts. However, by looking the Fig. 6(b), we can see that the small standard deviation of the MPS gain ratios corresponding to the fine scales (smaller than 256 μm) highlights a high repeatability.

Lastly, despite the promising results in the small scales compared to the 261X (Type II), the 2970 belt (Type III) action is limited to scales lower than 1.024 mm. This is mainly due to the orientation of its structure on the backing. We find that the minimum amplitude of the MPS corresponds approximately to the transversal spacing of the half-spherical structures as depicted in Fig. 7.

3.4. Specific energy

In order to better understand the influence of abrasive structures on the activation of the fundamental abrasion mechanisms (cutting plowing and sliding), an energetic analysis is performed by calculating the specific energy of the belt finishing. By definition, the specific energy represents the quantity of energy necessary to remove an elementary volume of materials from the workpiece. The overall value of this physical variable includes simultaneously the components induced by cutting action, plowing, sliding and frictional dissipation [10,11]. From an energetic point of view, an abrasive machining process is efficient if material is removed quickly with low energy consumption. Note that only the energy component due to cutting is expended by material removal which corresponds to the minimum finishing energy required. Here, the specific energy is calculated from the following

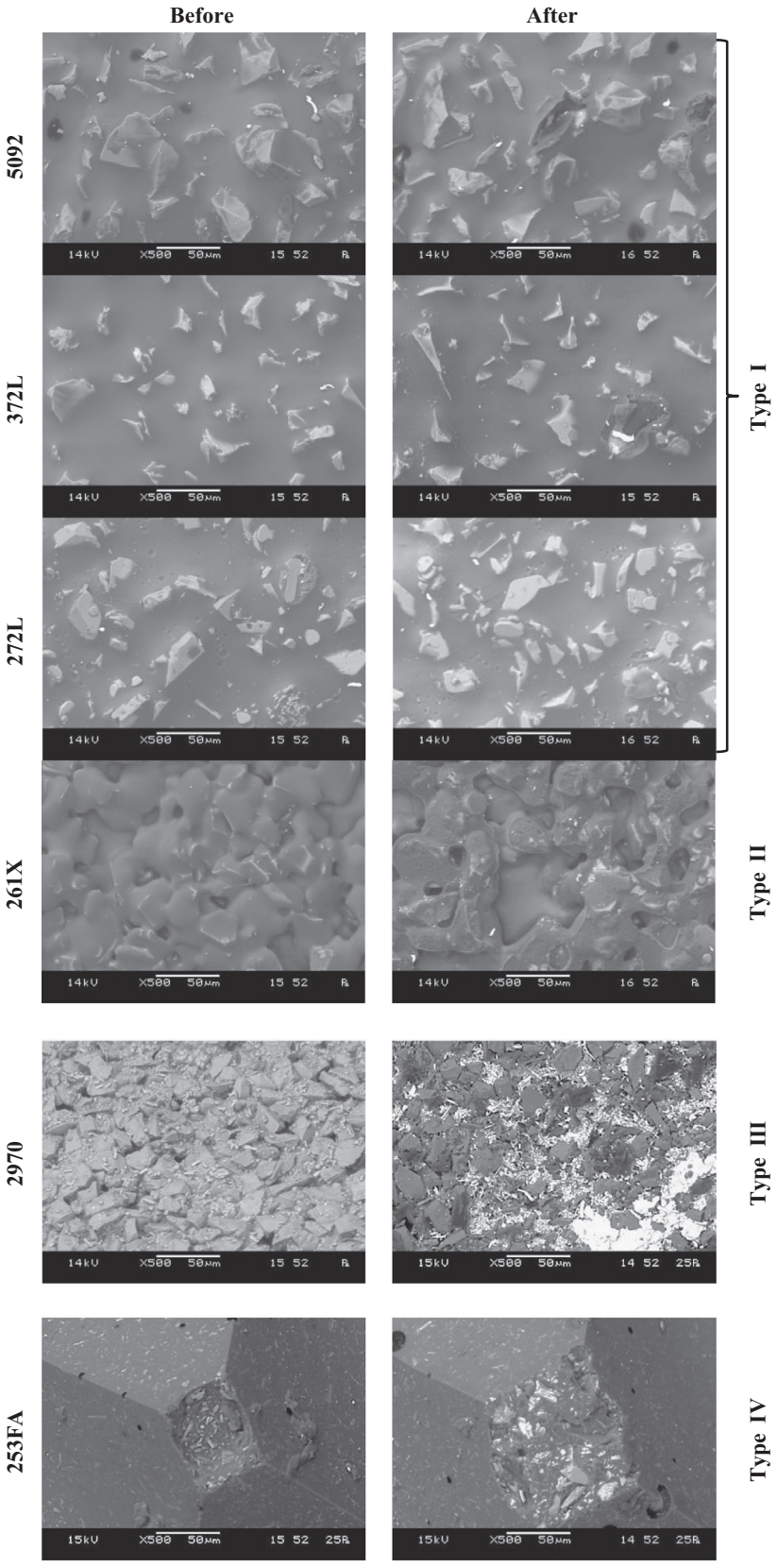

Fig. 3. SEM micrographs of initial and worn abrasive belts.

equations:

$$E_s = \frac{\Delta P \times t_c}{\Delta V} \tag{3}$$

$$\Delta V = \pi \times \left[R^2 - (R - 10^{-3} \times \Delta h)^2\right] \times L \tag{4}$$

where the Δh parameter (removal thickness) is based on the difference between the areas under the bearing curve (Abbot Curve) coming from the profiles before and after belt finishing [11,12]. It is approximated using ISO 13565 parameters (R_{pk}, R_k, R_{vk}, Mr1 and Mr2) by the following equations:

$$\Delta h = h_{initial} - h_{final} \tag{5}$$

$$h = \frac{1}{100}\left[\left(\frac{R_{pk}}{2} + (R_k + R_{vk})\right)Mr1 + \left(R_{vk} + \frac{R_k}{2}\right)(Mr2 - Mr1) + \left(\frac{R_{vk}}{2}\right)(100 - Mr2)\right] \tag{6}$$

These equations are based on the assumption that total surface depth is not removed when a small amount of wear occurs (removal thickness $< R_z$), which is the case in belt finishing when time cycle and grit size are small. Fig. 8 shows the average specific energy and removal thickness according to the belt models.

These results are in correlation with all the previous observations. The Type III belt exhibits the most important specific energy (about twice as important as the other types) while the removal thickness is very low. Once again we observe that belt finishing is not robust when this belt is used. Here the plowing and sliding seem to be the main mechanisms, which can be explained by the chip saturation of the structure, the small contact area, and the grit orientations (see Fig. 3). The results concerning the Type II belt also confirm what we have seen previously with the analysis of the R_{pk}, R_k and R_{vk} gain ratio. This belt structure does not ensure the same indentation depth on the workpiece surface as the Type I and IV belts. Here, micro-cutting, sliding and plowing mechanisms seem to be mixed.

Finally, the specific energy corresponding to the belt finishing with the 272L belt is slightly higher than the specific energy corresponding to the belt finishing with the two others Type I belts. This result may seem counter-intuitive given that this belt is denser than the 372L. However, it was previously observed that

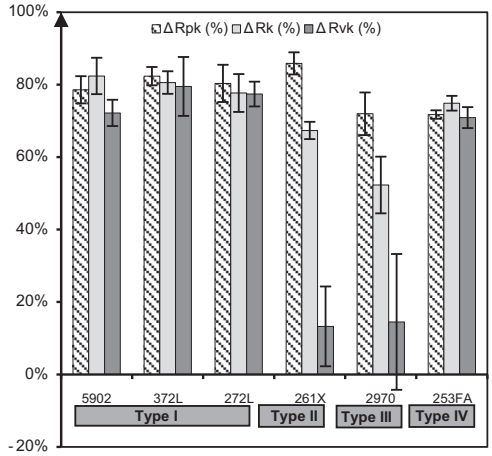

Fig. 4. Functional roughness R_{pk}, R_k and R_{vk} gain ratios.

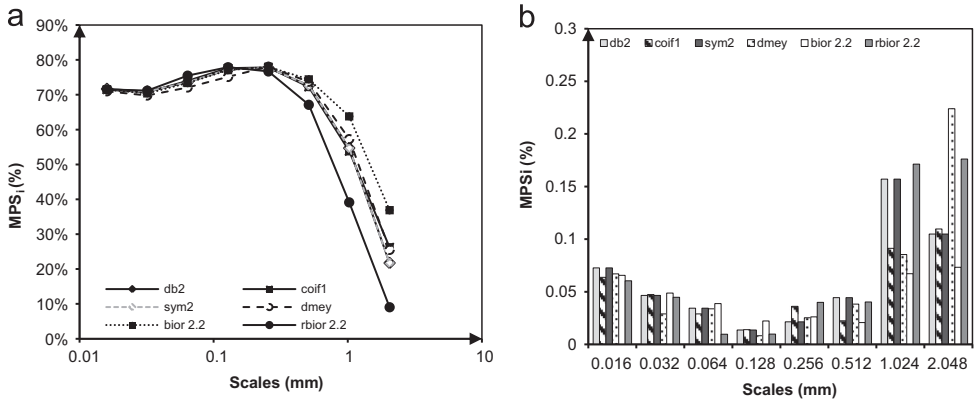

Fig. 5. Effect of wavelet function on the Multiscale Process Signature gain ratio (a) and standard deviations (b).

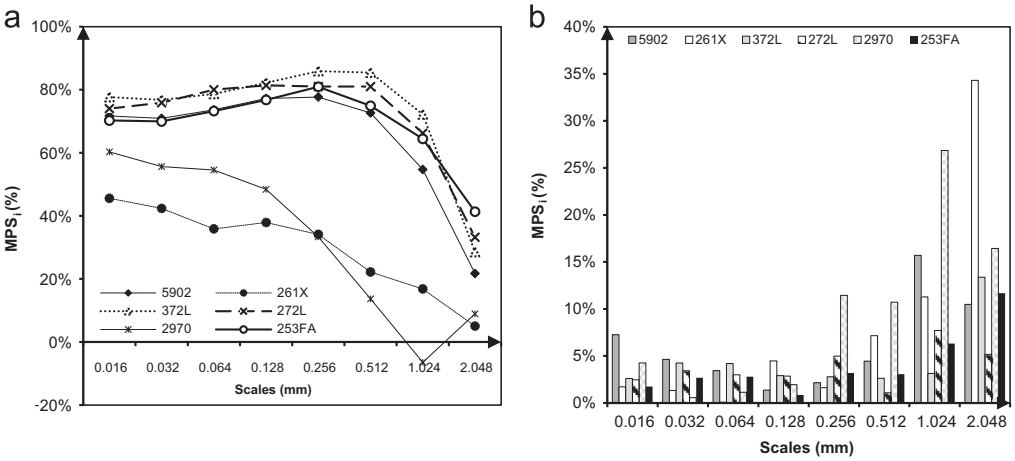

Fig. 6. Multiscale Process Signature gain ratio (a) and standard deviation of MPS$_i$ (%) (b).

the 272L's grits have a flatter orientation and less sharp cutting edges. Consequently, we see experimentally that the cutting edge profile here is more predominate than the grit density in order to reduce specific energy. In addition, irrespective Type I belt, micro-cutting is the main activated mechanism. Moreover, we observe that the Type IV belt has a better standard deviation than the Type I belt structure. Consequently, it seems that this structure improves the process repeatability of belt finishing, especially concerning the removal thickness.

3.5. Global belt finishing process efficiency

One of the ways to simply describe the global belt finishing process efficiency of each abrasive structure is to compute their relevance according to three criteria:

- The functional gain of the obtained surface, which is transcribed here through a global parameter evaluated from eq. (7). Note that in a lubricated contact such as in crankshaft bearings, the targeted roughness finish must offer the smallest peak (R_{pk}) and core height (R_k) in order to avoid the solid contact between the antagonist workpiece roughness while offering the deepest valleys (R_{vk}) to maintain lubricant in contact (particularly in a boundary and mixed lubrication regime [13]). Consequently, the higher the functional gain, the more the surface is functionally relevant.

$$Functional\ gain = \frac{\left(\frac{{R_{pk}}^{initial} + {R_k}^{initial}}{{R_{vk}}^{initial}}\right) - \left(\frac{{R_{pk}}^{final} + {R_k}^{final}}{{R_{vk}}^{final}}\right)}{\left(\frac{{R_{pk}}^{initial} + {R_k}^{initial}}{{R_{vk}}^{initial}}\right)} \quad (7)$$

- The repeatability criteria which represent the standard deviation of the *Functional gain*.
- The average specific energy which has been calculated above.

Finally, by plotting these three criteria in a normalized way (by dividing by the maximum value of each criterion), we are able to discern features associated with the belt structure in the belt finishing process.

This is illustrated in Fig. 9. We remark that the Type II structure (261X) leads to a good functionality while having one of the lowest repeatability errors. This trend allows for the reduction of roughness asperities without decreasing the valley depths. From this point of view, Type I and Type IV belts seem less efficient in that they are unable to preserve the valleys depth.

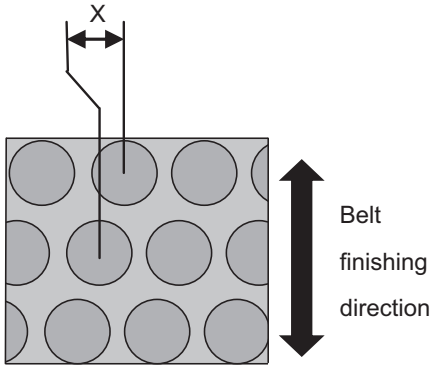

Fig. 7. 2970 belt's transversal spacing.

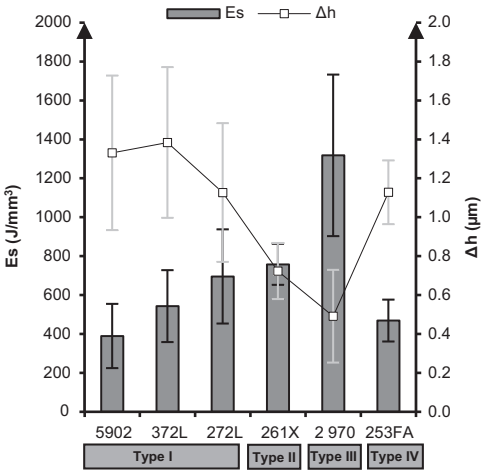

Fig. 8. Average specific energy E_s and removal thickness Δh.

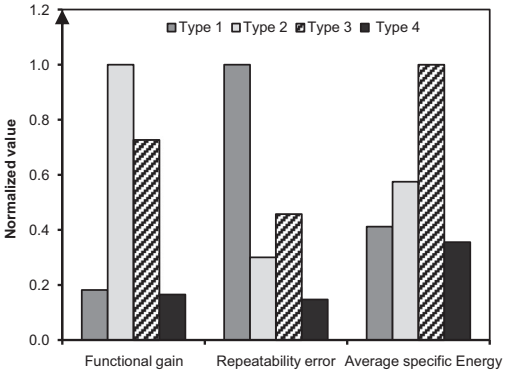

Fig. 9. Belt structure relevance for functionality issue.

4. Conclusions

In this paper, we consider the multiscale analysis of belt structure effects during the belt finishing of cylindrical hardened steel workpieces. Four morphologies of abrasive belts are considered. The analysis of the belt structure's impact is based on SEM characterization, functional roughness measurements, Multiscale Process Signature identification and an energetic process assessment. The results show that the belt structure plays an essential role in belt wear and belt finishing. This is, therefore, an important characteristic that must be taken into account for the development and selection of abrasive belts.

Particularly, we have found that the Type III belt structure comprised of half-spherical shaped agglomerates could limit the belt work in scales close to the transversal spacing between two successive half-spherical agglomerates. Consequently, it appears that there is a narrow link between the shapes' orientation on the backing and the actived roughness scales.

The introduction of global criteria has particularly shown the interest of the Type II structure. We have seen that its morphology with slanting cutting edges consistently allows for a significant reduction in the asperities' height without acting on the valley depth. Without modifying belt finishing cycle time, a functional gain can be obtained.

Further studies will be done in order to compare the wear dynamic of these different abrasive belt morphologies and their durability.

References

[1] M. El Mansori, E. Sura, P. Ghidossi, S. Deblaise, T. Dal, H. Khanfir, Toward physical description of form and finish performance in dry belt finishing process by a tribo-energetic approach, J. Mater. Process. Technol. 182 (2007) 498–511. http://dx.doi.org/10.1016/j.jmatprotec.2006.09.009.

[2] K. Holmberg, P. Andersson, A. Erdemir, Global energy consumption due to friction in passenger cars, Tribol. Int. 47 (2012) 221–234. http://dx.doi.org/10.1016/j.triboint.2011.11.022.

[3] M.C. Shaw, Principles of Abrasive Processing, Oxford Science Publications, Clarendon Press, Oxford, 1996.

[4] H. Hamdi, M. Dursapt, H. Zahouani, Characterization of abrasive grain's behavior and wear mechanisms, Wear 254 (2003) 1294–1298. http://dx.doi.org/10.1016/S0043-1648(03)00158-3.

[5] L. De Chiffre, P. Lonardo, H. Trumpold, D.A. Lucca, G. Goch, C.A. Brown, et al., Quantitative characterisation of surface texture, CIRP Ann. – Manuf. Technol. 49 (2000) 635–652.

[6] L. Sabri, S. Mezghani, M. El Mansori, H. Zahouani, Multiscale study of finish-honing process in mass production of cylinder liner, Wear. 271 (2011) 509–513. 10.1016/j.wear.2010.03.026.

[7] S. Mezghani, M. El, A. Massaq, P. Ghidossi, Correlation between surface topography and tribological mechanisms of the belt-finishing process using multiscale finishing process signature, C. R. Mecanique. 336 (2008) 794–799. 10.1016/j.crme.2008.09.002.

[8] M. El Mansori, S. Mezghani, L. Sabri, H. Zahouani, On concept of process signature in analysis of multistage surface formation, Surf. Eng. 26 (2010) 216–223.

[9] M. Bigerelle, G. Guillemot, Z. Khawaja, M. El Mansori, J. Antoni, Relevance of wavelet shape selection in a complex signal, Mech. Syst. Signal Process. 41 (2013) 14–33. http://dx.doi.org/10.1016/j.ymssp.2013.07.001.

[10] S. Mezghani, M. El Mansori, E. Sura, Wear mechanism maps for the belt finishing of steel and cast iron, Wear. 267 (2009) 86–91. http://dx.doi.org/10.1016/j.wear.2008.12.113.

[11] S. Mezghani, I. Demirci, M. Yousfi, M. El Mansori, Running-in wear modeling of honed surface for combustion engine cylinder liners, Wear. (2013) 1–10. 10.1016/j.wear.2013.01.026.

[12] R. Kumar, S. Kumar, B. Prakash, A. Sethuramiah, Assessment of engine liner wear from bearing area curves, Wear 239 (2000) 282–286.

[13] P. Pawlus, A study on the functional properties of honed cylinders during running-in, Wear 176 (1994) 247–254.